Acta Crystallographica Section B
Structural Science
ISSN 0108-7681

Structure of a high-pressure phase of vanadium pentoxide, β-V_2O_5

V. P. Filonenko,[a] M. Sundberg,[b]* P.-E. Werner[b] and I. P. Zibrov[c]

[a]Institute for High Pressure Physics, Russian Academy of Sciences, Troitsk, 142190 Moscow Region, Russia, [b]Department of Inorganic and Structural Chemistry, Arrhenius Laboratory, Stockholm University, SE-106 91 Stockholm, Sweden, and [c]Institute of Crystallography, Russian Academy of Sciences, 117333 Moscow, Russia

Correspondence e-mail: marsu@inorg.su.se

Received 19 March 2004
Accepted 25 May 2004

A high-pressure phase of vanadium pentoxide, denoted β-V_2O_5, has been prepared at P = 6.0 GPa and T = 1073 K. The crystal structure of β-V_2O_5 has been studied by X-ray and neutron powder diffraction, and high-resolution transmission electron microscopy. The V atoms are six-coordinated within distorted VO_6 octahedra. The structure is built up of quadruple units of edge-sharing VO_6 octahedra linked by sharing edges along [010] and mutually connected by sharing corners along [001]. This arrangement forms layers of V_4O_{10} composition in planes parallel to (100). The layers are mutually held together by weak forces. β-V_2O_5 is metastable and transforms to α-V_2O_5 at 643–653 K under ambient pressure. Structural relationships between β- and α-V_2O_5, and between β-V_2O_5 and B-Ta_2O_5-type structures are discussed. The high-pressure β-V_2O_5 layer structure can be considered as the parent of a new series of vanadium oxide bronzes with cations intercalated between the layers.

1. Introduction

The thermodynamically stable modification of vanadium pentoxide, denoted α-V_2O_5, can be described as a two-dimensional layer structure of edge- and corner-sharing, square VO_5 pyramids (Byström *et al.*, 1950). The intercalation of transition metal complexes and molecular compounds in the open structure of V_2O_5 has been extensively investigated for many years. By chemical or electrochemical de-intercalation of lithium from the γ'-LiV_2O_5 bronze, a metastable polymorph of V_2O_5, denoted γ'-V_2O_5, has been prepared by Cocciantelli *et al.* (1991). The latter structure is built up of puckered layers of edge-sharing distorted VO_5 pyramids. The linkage of the pyramids within the layers is approximately the same as that in γ'-LiV_2O_5, but differs from that in the α-V_2O_5 structure.

Only a few high-pressure investigations of vanadium pentoxide have been published (Minomura & Drickamer, 1961; Suzuki *et al.*, 1977; Volkov *et al.*, 1988; Grzechnik, 1998; Loa *et al.*, 2001). The first X-ray diffraction pattern of a high-pressure modification of V_2O_5 (prepared under the following conditions: P = 4.0–6.0 GPa and T = 923 K) was obtained by Suzuki *et al.* (1977). Later, Volkov *et al.* (1988) found that the high-pressure variety of V_2O_5 (denoted β-V_2O_5) was formed in the pressure region 3.5–9.0 GPa at a temperature of 873 K. The X-ray diffraction pattern of β-V_2O_5 has been published (ICDD-PDF 45–1074), but no structure model has been presented so far. Recent Raman spectroscopy studies of the effect of high

Table 1
Experimental details for β-V_2O_5.

	(I)	(II)
Chemical formula	V_2O_5	V_2O_5
M_r	181.88	181.88
Cell setting, space group	Monoclinic, $P2_1/m$	Monoclinic, $P2_1/m$
a, b, c (Å)	7.1140 (2), 3.5718 (1), 6.2846 (2)	7.1140 (2), 3.5718 (1), 6.2846 (2)
β (°)	90.069 (3)	90.069 (3)
V (Å^3)	159.69 (1)	159.69 (1)
Z	2	2
D_x (Mg cm^{-3})	3.783 (1)	3.783 (1)
Radiation type	Neutrons	Cu $K\alpha_1$
Temperature (K)	293	293
Specimen form, color	Cylindrical diameter 9 mm, dark red	Flat sheet, dark red
Specimen preparation cooling rate (K min^{-1})	6000	6000
Specimen preparation pressure (kPa)	6×10^6	6×10^6
Specimen preparation temperature (K)	1073	1073
Data collection		
Diffractometer	Neutron powder, NPD	Stoe Stadi/P
Data collection method	Specimen mounting: packed powder pellet; mode: Debeye–Sherrer; scan method: step	Specimen mounting: drifted powder on Kapton film; mode: transmission; scan method: step
Absorption correction	None	None
2θ (°)	$2\theta_{min}$ = 8.153, $2\theta_{max}$ = 133.433, increment = 0.08	$2\theta_{min}$ = 5.0, $2\theta_{max}$ = 88.94, increment = 0.02
Refinement		
Refinement on	I_{net}	I_{net}
R factors and goodness-of-fit	R_p = 0.030, R_{wp} = 0.040, R_{exp} = 0.024, S = 1.07	R_p = 0.015, R_{wp} = 0.020, R_{exp} = 0.029, S = 1.07
Wavelength of incident radiation (Å)	1.47	1.54056
Excluded regions	None	None
Profile function	Gaussian	Pseudo-Voigt
No. of parameters used	68	
$(\Delta/\sigma)_{max}$	0.04	0.04
D†	1.074	0.848

Computer programs: *GSAS* (Larson & Von Dreele, 1987). † D = Durbin–Watson statistic D value according to Hill & Flack (1987).

pressures on the structure of α-V_2O_5 have suggested that a structural transformation to a three-dimensional V_2O_5 network occurs at $\sim$ 7 GPa (Grzechnik, 1998; Loa *et al.*, 2001).

During the last few years we have been interested in exploring the influence of high pressure and high temperature on the structures of binary and ternary transition metal oxides, and have developed a high-pressure synthesis method for the tungsten oxygen and niobium oxygen systems (Zibrov *et al.*, 1998). We have recently expanded these studies to include vanadium pentoxide. In this paper we present the crystal structure of the high-pressure phase, β-V_2O_5, studied by X-ray and neutron powder diffraction and high-resolution transmission electron microscopy. The structure was refined by a combination of X-ray and neutron diffraction data, using Rietveld analysis. A second high-pressure modification of vanadium pentoxide, B-V_2O_5, isostructural with B-Nb_2O_5, was recently identified in samples prepared at P = 8.0–8.5 GPa (Filonenko & Zibrov, 2001). A structure determination of B-V_2O_5 will be published separately.

2. Experimental

V_2O_5 powder (99.9% purity) was pressed into pellets, which were wrapped up in tungsten foil to avoid chemical reaction between the specimen and the surrounding high-pressure cell material, especially the graphite heater. A description of the 'toroid'-type high-pressure chamber and the experimental synthesis procedure has been published by Zibrov *et al.* (1998). The specimens used here were obtained under the following conditions: pressure P = 6.0 GPa and temperature T = 1073 K. The final product had a dark red color.

For the transmission electron microscopy (TEM) studies, a small amount of the sample was crushed in an agate mortar under *n*-butanol. A few drops of the suspension were put on a Cu grid covered by a perforated carbon film. Electron diffraction (ED) patterns and high-resolution transmission electron microscopy (HRTEM) images were taken of thin crystal fragments on the Cu grid in a Jeol 3010 microscope operated at 300 kV and equipped with a double-tilt goniometer stage with tilt angles $\pm$ 10–20°.

2.1. Structure determination and thermal analysis studies

X-ray powder photographs were recorded in a subtraction-geometry Guinier–Hägg focusing camera with strictly monochromated Cu $K\alpha_1$ radiation. Si was used as an internal standard. There were 34 observed lines in the XRD pattern ($5 < 2\theta < 90°$). The auto-indexing program *Treor*90 (Werner *et al.*, 1985) was used to find the lattice parameters. All lines could be indexed and refined with an orthorhombic unit cell with the dimensions: a = 7.1229 (7), b = 6.2936 (9) and c = 3.5753 (3) Å, (V = 160.27 Å^3). From the systematic absence conditions found, the four space groups $P222_1$, $P222$, $Pmm2$ and $Pmmm$ were regarded as possible.

X-ray diffraction data for structure determination were collected on a Stoe Stadi/P diffractometer with a flat rotating thin (< 0.3 mm) sample in the symmetric transmission mode. A symmetric focusing germanium monochromator (focal distance = 440 mm) was used to give pure Cu $K\alpha_1$ radiation. The diffraction data were collected with a small linear position-sensitive detector (PSD) covering 6.4° in 2θ. The PSD was moved in steps of 0.2°, 300 *s* per step, thus giving an average intensity of 32 measurements at each 2θ position. This

procedure was used in order to eliminate errors depending on the intensity calibration curve of the detector (Goebel, 1979). The 2θ range measured was $5 < 2\theta < 90°$. The peak shapes could be described by a symmetric, or nearly symmetric, pseudo-Voigt function.

The contribution from the V atoms (46 electrons in the formula unit) to the X-ray scattering is approximately the same as that of the O atoms (40 electrons). On the other hand, the scattering of neutrons from V atoms ($b = -0.0382$) is insignificant in comparison to scattering from oxygen ($b = 0.581$), which allows one to locate O in the unit cell with higher accuracy. For this reason, neutron diffraction data were collected at the reactor in Studsvik (Sweden). The 2θ range measured was $4 < 2\theta < 140°$, step size 0.08°, $\lambda = 1.47$ Å. The peak shapes were described by a modified Gaussian function.

Both data sets (X-ray and neutron) were used for structure solution and refinement using the programs *EXPO*2001 (Altomare *et al.*, 1999) and *GSAS* (Larson & Von Dreele, 1987). We could not find any reasonable model with orthorhombic symmetry, which strongly suggests that the real symmetry is lower than orthorhombic. From the assumption that the symmetry is monoclinic, with the 3.57 Å axis as the unique b axis and ($0k0$) reflections present for $k = 2n$ only, we found a reasonable solution in the centrosymmetric space group $P2_1/m$. A few triclinic models were also tested without any improvement of the structure refinement.

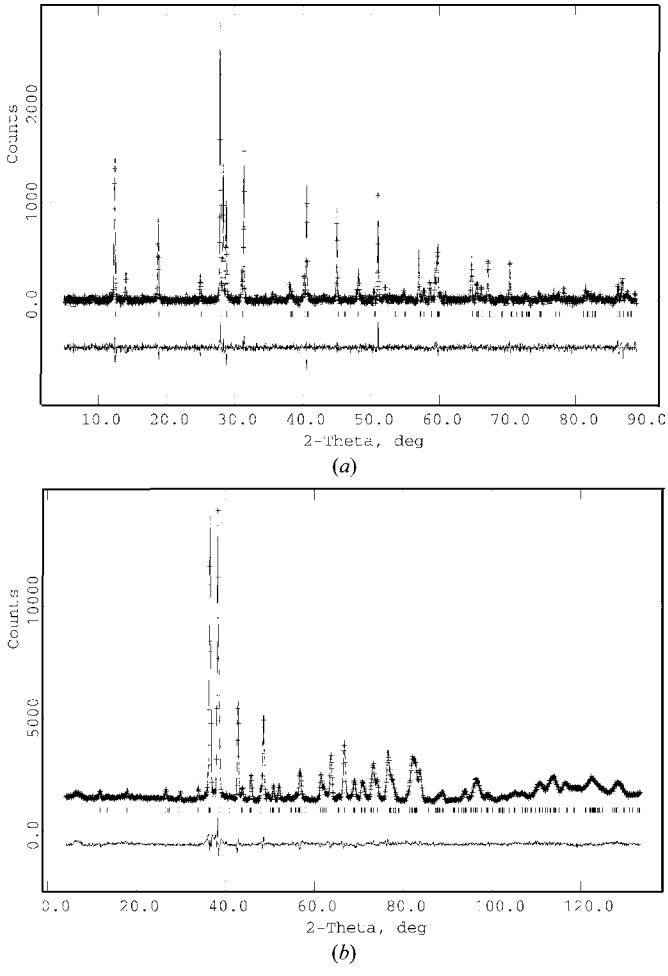

Figure 1
Rietveld refinement of β-V_2O_5. Observed (+), calculated (solid line) and the difference between observed and calculated (bottom curve) powder diffraction profiles are shown. The positions of all the allowed Bragg reflections are indicated by the row of vertical tick marks. (*a*) X-ray data; (*b*) neutron data.

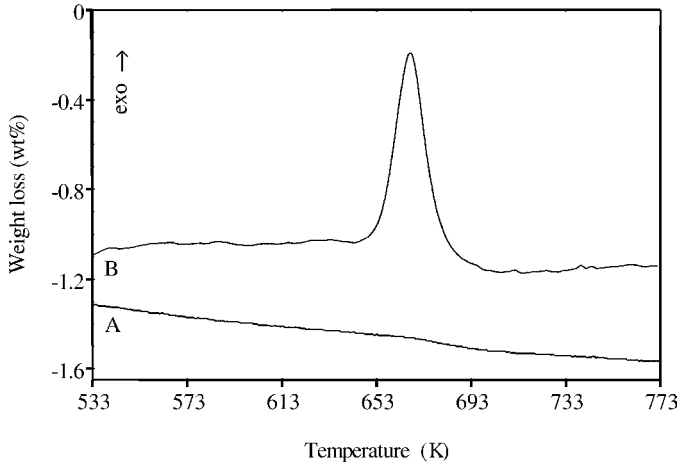

Figure 2
TG (*A*) and DTA (*B*) curves of β-V_2O_5 heated in an O_2 atmosphere.

The structure model was then refined by the Rietveld method with the program *GSAS*, using both the X-ray and neutron data sets. The observed data and the differences between observed and calculated data are shown in Fig. 1. The crystal data and details about the data collection and structure refinement are reported in Table 1. The positional atomic parameters and the isotropic displacement parameters have been deposited.[1] The higher R_F value for the X-ray data in Table 1 is probably due to the strong fluorescence of the V atoms induced by copper radiation and to the absorption effects caused by the transmission geometry of the diffractometer. The calculated density, $\rho_{calc} = 3.783$ g cm^{-3} for $Z = 2$, is in a fairly good agreement with the pycnometrically measured value, $\rho_{obs} = 3.603$ (7) g cm^{-3}.

Thermoanalysis studies of β-V_2O_5 were carried out in two instruments; a Perkin Elmer TGA-7 apparatus (TG) and a Setaram Labsys 1600 (DTA). β-V_2O_5 samples were heated up to 773 K in an oxygen atmosphere at a scan rate of 5 K min^{-1}. The curves are plotted in Fig. 2. The DTA curve (marked *B*) shows a strong exothermic peak in the temperature region 643–653 K which is associated with the phase transformation β- $\Rightarrow$ α-V_2O_5. The corresponding TG curve (marked *A*) shows no increase in weight, thus indicating that the sample is V_2O_5. The X-ray powder patterns taken before and after the TGA run confirmed the phase transition.

2.2. Electron microscopy study

The lattice parameters obtained from the selected-area electron diffraction (SAED) study agreed with the unit-cell

[1] Supplementary data for this paper are available from the IUCr electronic archives (Reference: SN0038). Services for accessing these data are described at the back of the journal.

dimensions obtained by X-ray diffraction and reported in Table 1. The SAED patterns displayed sharp spots, indicating well ordered crystals. No streaking or superlattice reflections could be seen in the patterns. The electron diffraction studies in combination with microanalysis did not show the presence of any impurity element in the examined crystals. The HRTEM images taken of thin β-V_2O_5 crystals aligned along [010] suggested an ordered structure with layers parallel to (100). Only a few isolated stacking faults were observed. The HRTEM study also showed that the β-V_2O_5 structure slowly decomposed to an amorphous phase due to the heat from the electron beam. From the latter results it was apparent that convergent-beam electron diffraction could not be used to prove the monoclinic symmetry of the metastable β-V_2O_5 phase.

2.3. Structure description

The selected interatomic distances listed in Table 2 show six-coordinated vanadium atoms, V1 and V2, within highly distorted VO_6 octahedra. The V atoms in the octahedra are off-center (see Figs. 3*a* and *b*), yielding the short bond distances V1—O1 = 1.649 and V2—O3 = 1.583 Å, the latter typical of a vanadyl group. Opposite to these short bonds are the long ones, V1—O2 2.308 and V2—O2 2.295 Å. The $V1O_6$ and $V2O_6$ octahedra are linked in pairs at $y = \frac{1}{4}$ and $y = \frac{3}{4}$. Every other pair along *b* is rotated through 180° and the pairs are then joined by edge sharing, thus forming the characteristic structural building unit of four edge-sharing octahedra in the β-V_2O_5 structure (see Fig. 3*c*). A similar block consisting of four edge-sharing octahedra has been denoted a quadruple unit by Rozier *et al.* (1996). The crystal structure of β-V_2O_5 can be described as built up of infinite chains of such quadruple units, sharing edges along the short *b* axis (Fig. 4). The chains are mutually linked by corner-sharing between two octahedra along **c**, thus forming two-dimensional layers of the composition V_4O_{10} in planes parallel to (100). The layers are mutually held together by weak forces as in the α-MoO_3 structure. The O3 atom, located at the boundary of the layer (see Figs. 3 and 4), is linked to V2 only and forms the shortest bond V2—O3 1.583 Å, which is thus the strongest vanadyl bond. The other short bond length mentioned above, V1—O1 1.649 Å, is involved in corner-sharing between the VO_6 octahedra of V1 and V2, which results in the bond lengths V1—O1 1.649 and V2—O1 2.060 Å. The latter distance is much shorter than the longest distance V2—O2 2.295 Å in the VO_6 octahedron of V2. The bond-valence calculations (Table 2) confirm the valence state of vanadium (V^{5+}) in β-V_2O_5.

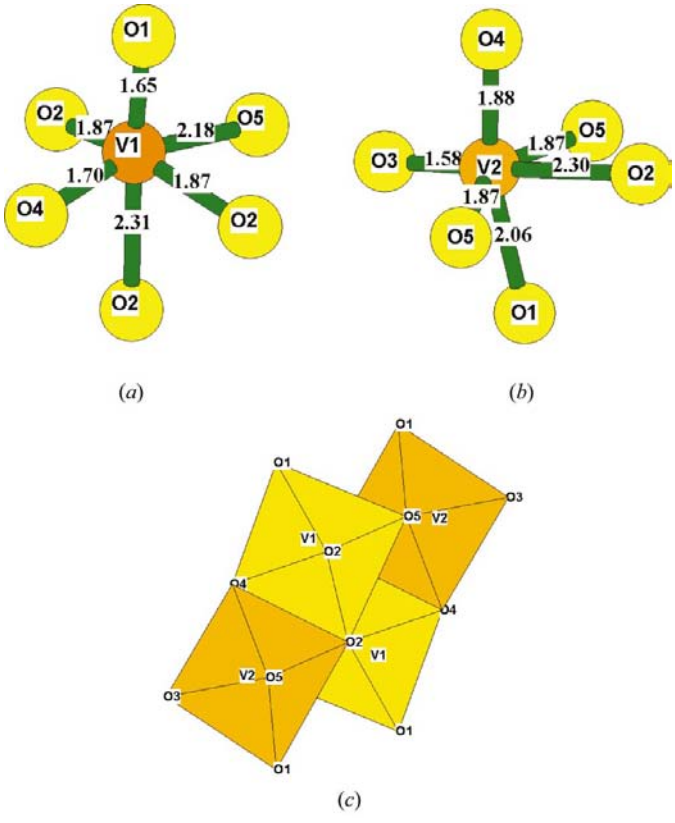

Figure 3
View of (*a*) $V1O_6$ and (*b*) $V2O_6$ coordination polyhedra. (*c*) A group of four edge-sharing VO_6 octahedra (quadruple unit) projected along *b* = 3.57 Å. All structure models were produced with *ATOMS* by Shape Software.

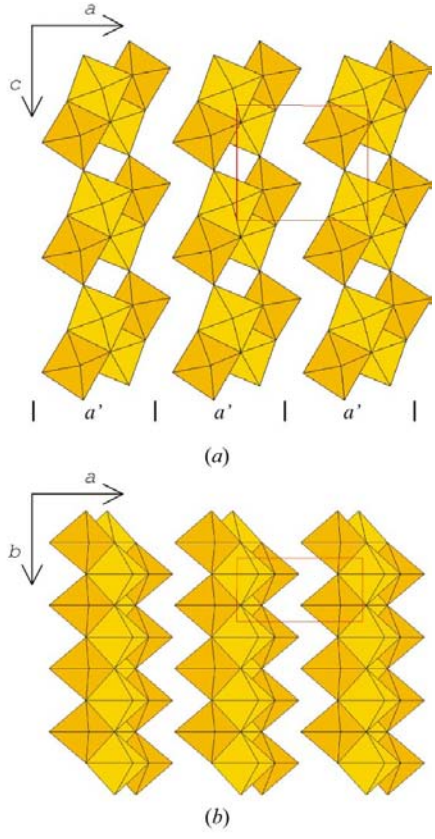

Figure 4
The crystal structure of β-V_2O_5 projected along (*a*) [010] and (*b*) [001].

Table 2
Selected interatomic distances, r_{ij} (Å), and the corresponding bond valences, s_{ij} (calculated with the parameters of Wills & Brown, 1999).

	r_{ij}	s_{ij}
V1—V1^{i}	3.301 (8)	
V1—V2	3.069 (8)	
V1—V2^{i}	3.249 (5)	
V1—O1^{i}	1.649 (6)	1.52
V1—O2	2.308 (6)	0.254
V1—O2^{i}	1.872 (2)	0.83
V1—O2^{i}	1.872 (2)	0.83
V1—O4	1.704 (7)	1.3
V1—O5^{i}	2.176 (6)	0.365
		Sum 5.099
V2—O1^{i}	2.060 (8)	0.495
V2—O2	2.295 (6)	0.266
V2—O3	1.583 (6)	1.812
V2—O4	1.882 (8)	0.819
V2—O5	1.871 (2)	0.834
V2—O5	1.871 (2)	0.834
		Sum 5.06
O1—O1^{i}	3.173 (7)	
O1—O2	2.758 (4)	
O1—O2^{i}	2.999 (7)	
O1—O3	3.047 (4)	
O1—O3^{i}	2.698 (5)	
O1—O4^{i}	2.636 (7)	
O1—O5	2.887 (5)	
O1—O5^{i}	2.602 (4)	
O2—O2^{i}	2.602 (7)	
O2—O4	2.644 (5)	
O2—O4^{i}	2.705 (4)	
O2—O5	2.529 (4)	
O2—O5^{i}	2.836 (7)	
O3—O3^{i}	2.838 (7)	
O3—O4	2.674 (7)	
O3—O4^{i}	2.919 (4)	
O3—O5	2.768 (4)	
O4—O5	2.720 (5)	

3. Discussion

The present structural analysis clearly shows that the V atoms in the high-pressure β-V_2O_5 modification must be considered as octahedrally six-coordinated, even if the distortion is considerable and essentially consists of an off-center displacement of the vanadium atoms towards one corner of the octahedron. This displacement is much less than in α-V_2O_5, where the longest V—O distance is 2.791 Å (Enjalbert & Galy, 1986). This means that the coordination number increases from five to six when the pressure is increased. Both modifications form layered structures, with the O atoms at the border of the layers linked to the V atoms with V═O double bonds of length 1.577 (α form) and 1.583 Å (β form), thus forming vanadyl groups. In α-V_2O_5 (a = 11.512, b = 3.564, c = 4.368 Å; Enjalbert & Galy, 1986) the two-dimensional layers consisting of corner- and edge-sharing VO_5 pyramids are parallel to (001) (Figs. 5*a* and *b*), whereas in β-V_2O_5 the two-dimensional layers are parallel to (100) and are built up of chains of edge-sharing quadruple units linked by sharing corners (Fig. 4). If the sixth O atom is included in the coordination polyhedron the α-V_2O_5 structure can be considered as a three-dimensional network of edge- and corner-sharing VO_6 octahedra (Figs. 5*c* and *d*). The relationship between the two modifications of V_2O_5 can be seen if the α-V_2O_5 structure is considered as built up from thin slabs of edge-sharing VO_6 octahedra. The slabs are two octahedra wide and are parallel to (100) and linked by corner-sharing. Every second slab is mirrored. The two slabs are denoted *a* and *b* in Fig. 5. In the β-V_2O_5 structure all slabs (marked *a*′ in Fig. 4) have the same orientation and are identical. As the stacking sequences and the arrangement of octahedra in the slabs differ between the two phases (*abab* in the α-form and *a*′*a*′*a*′*a*′ in the β-modification), the transition process α-V_2O_5 to β-V_2O_5 can be explained by a conversion of a *b* layer into an *a* layer in the α-form followed by a compression of the α-V_2O_5 structure along the *c*-axis by crystallographic shear (CS). The conversion is equivalent to a 180° rotation of the *b* layer around the *a* axis. A similar transition of a *b*-slab to an *a*-slab has previously been suggested for the phase transformation α-MoO_3 (stable ambient-pressure phase) to MoO_3 II (high-pressure phase; McCarron III & Calabrese, 1991). A hypothetical model of the transition of an α-V_2O_5 slab (marked *a*) to a β-V_2O_5 slab (marked *a*′) is illustrated in Fig. 6. The compression by crystallographic shear along the *c* axis means that the long V—O distance (2.791 Å) will be shortened. The formation of chains of edge-sharing octahedra by CS will result in a loss of oxygen, which will be compensated by the break-up of the structure in slabs (*a*′) where the O atoms at the border of the layers are linked to the vanadium atoms with V═O double bonds. The combination of high pressure and high temperature during the synthesis seems to be necessary for the conversion of *b* layers into *a* layers by small displacements of the V and O atoms and the following compression process. The calculated densities 3.783 g cm^{-3} (β-form) and 3.37 g cm^{-3} (α-form) also show that the structure of β-V_2O_5 is much more dense than that of α-V_2O_5. It should also be mentioned that our thermogravimetric results indicate that β-V_2O_5 is a metastable, stoichiometric compound, which transforms to α-V_2O_5 at 643–653 K. β-V_2O_5 can thus be considered as a high-pressure modification of V_2O_5.

Figs. 7(*a*–*c*) show that the β-V_2O_5 structure can alternatively be described as built up of layers stacked parallel to the *ac*-plane. The layers (at y = 1/4 and y = 3/4) consist of isolated strings composed of pairs of edge-sharing VO_6 octahedra linked by corners along the *c* axis. The strings are mutually linked by edge-sharing along **b** (Fig. 4*b*). Similar strings in two planes build up the structures of the high-pressure phases *B*-Ta_2O_5 and *B*-Nb_2O_5 (Zibrov *et al.*, 2000) as can be seen in Fig. 7(*d*)–(*f*). The orientations of the pairs of edge-sharing octahedra in the strings differ, however. In the *B*-Ta_2O_5-related structures the pairs are mutually linked by sharing corners, in such a way that rutile-like slabs are formed (Fig. 7*d*). The crystal structure of the *B*-phase is denser than that of β-V_2O_5. The similarities between the two structures indicate that the *B*-form could be obtained from the β-phase. The strings in *B*-Ta_2O_5 (in Figs. 7*e* and *f*) can be obtained from the β-phase by tilting the pairs in the strings (Figs. 7*b* and *c*) about 45° in opposite directions. It thus seems very likely that the increased pressure during the high-pressure/high-temperature synthesis will result in a second phase transfor-

mation from β-V_2O_5 to B-V_2O_5. This was recently verified by our X-ray diffraction studies of samples, prepared at P = 8.0 GPa. The X-ray results showed that B-V_2O_5 is isostructural with B-Nb_2O_5 (Zibrov *et al.*, 1998) and that the V atom is six-coordinated in the shape of a fairly regular VO_6-octahedron with V—O distances in the range 1.64–2.15 Å (Filonenko *et al.*, 2004). The change in vanadium coordination from five- to sixfold with increasing pressure has previously been proposed by Grzechnik (1998) and Loa *et al.* (2001) from their Raman spectroscopy studies of V_2O_5.

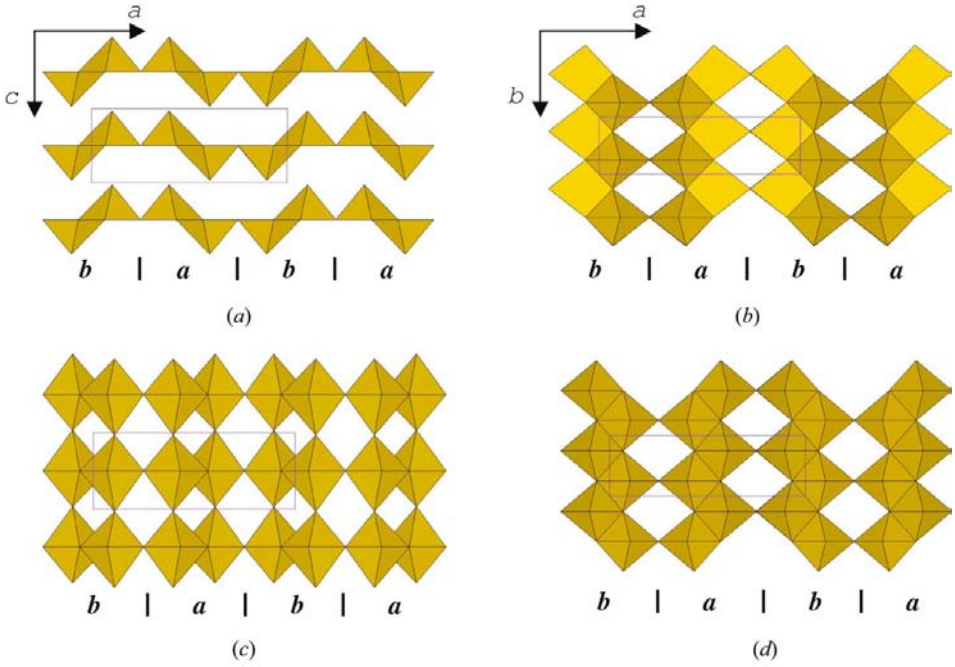

Figure 5
The crystal structure of α-V_2O_5 projected along [010] in (*a*) and (*c*), and [001] in (*b*) and (*d*). The V atoms are five-coordinated as VO_5 square pyramids in (*a*) and (*b*), whereas they are described as six-coordinated in (*c*) and (*d*).

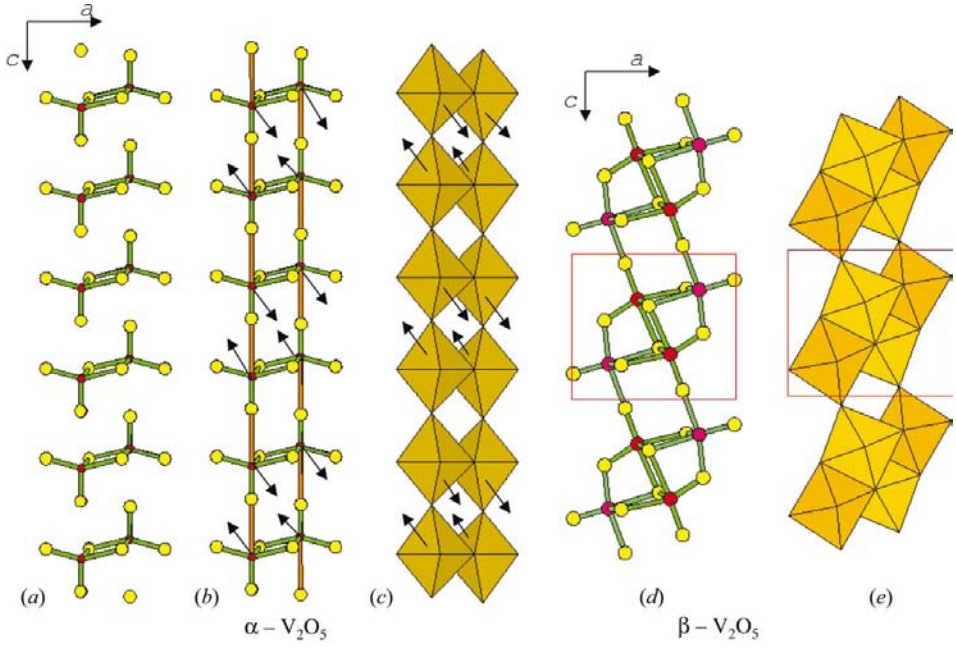

Figure 6
Thin slabs of α-V_2O_5 and β-V_2O_5 projected along the b = 3.57 Å axis. Hypothetical model showing the transformation from an a slab in α-V_2O_5 to an a' slab in β-V_2O_5. The arrows in (*b*) and (*c*) indicate the formation of the CS groups in (*d*) and (*e*).

The crystal structure of the present high-pressure form of V_2O_5 has been predicted as a possible structure of a silver vanadium bronze of the composition $Ag_xV_4O_{10}$ ($x \leq 2$) with the Ag atoms located between the V_4O_{10} double layers. Rozier *et al.* (1996) derived the latter structure from the silver vanadium oxide bronze structure of β-$Ag_4V_4O_{12}$, using crystallographic shear mechanisms to explain the reduced oxygen content in the starting product. However, a silver vanadium bronze with the predicted structure has not yet been found. A few years ago, Chirayil *et al.* (1997) reported the first vanadium oxide, *TMA*V_8O_{20} (*TMA* = tetramethylammonium), as being isostructural with the predicted structure of $Ag_xV_4O_{10}$ ($x \leq 2$) with the large *TMA* cations located between the V_4O_{10} double layers. The vanadium oxide layers in *TMA*V_8O_{20} and β-V_2O_5 are thus also isotypic. The unit-cell parameters, b = 3.5931 (3) and c = 6.3175 (5) Å, reported for *TMA*V_8O_{20} are in a good agreement with the corresponding ones of β-V_2O_5 given in Table 1. The long a axis, 23.655 Å in *TMA*V_8O_{20}, is due to the intercalation of the large *TMA* cations into the layer structure of β-V_2O_5. The structure of the high-pressure β-V_2O_5 modification can thus be considered as the parent structure for a new series of vanadium oxide bronzes consisting of infinite double layers of the composition V_4O_{10} with positive ions intercalated.

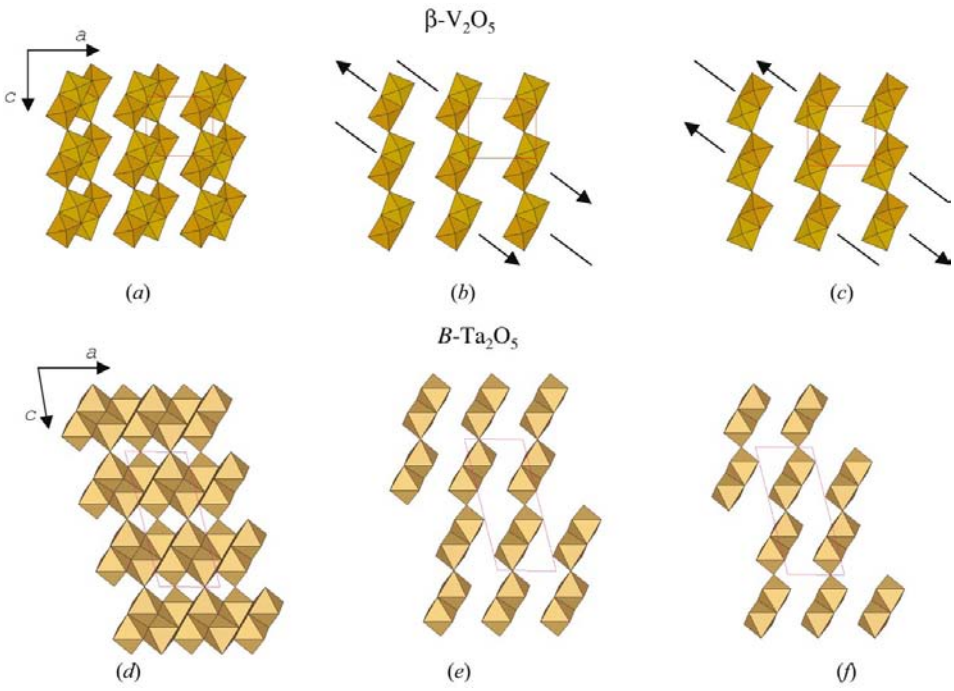

Figure 7
The crystal structure of β-V_2O_5 projected along [010] in (*a*)–(*c*). The two layers at $y = \frac{1}{4}$ and $y = \frac{3}{4}$ are shown in (*b*) and (*c*). The layers are connected by edge-sharing along **b**. The arrows denote a possible tilt of the pairs in the strings from β to *B*. The crystal structure of *B*-Ta_2O_5 is projected along [010] in (*d*)–(*f*). The two layers at $y = \frac{1}{4}$ and $y = \frac{3}{4}$ are shown in (*e*) and (*f*). The layers are mutually linked by corner-sharing so that rutile-like slabs are formed; see (*d*).

We want to thank Dr R. McGreavy at NFL, Studsvik, for providing facilities for the neutron diffraction work and Mr H. Rundlöf for the collection of the neutron diffraction data. We are grateful to Dr K. Jansson for valuable assistance with the thermal analysis studies of β-V_2O_5. Financial support from the Royal Swedish Academy of Sciences, the Swedish Research Council and the Russian Foundation for Basic Research, grant N 01-03-32457 is gratefully acknowledged.

References

Altomare, A., Burla, M. C., Camalli, M., Carrozzini, B., Cascarano, G. L., Giacovazzo, C., Guagliardi, A., Moliterni, A. G. G., Polidori, G. & Rizzi, R. (1999). *J. Appl. Cryst.* **32**, 339–340.

Byström, A., Wilhelmi, K.-A. & Brotzen, O. (1950). *Acta Chem. Scand.* **4**, 1119–1130.

Chirayil, T., Zavalij, P. Y. & Whittingham, M. S. (1997). *J. Mater. Chem.* **7**, 2193–2195.

Cocciantelli, J. M., Gravereau, P., Doumerc, J. P., Pouchard, M. & Hagenmuller, P. (1991). *J. Solid State Chem.* **93**, 497–502.

Enjalbert, R. & Galy, J. (1986). *Acta Cryst.* C**42**, 1467–1469.

Filonenko, V. P., Sundberg, M. & Zibrov, I. P. (2004). In preparation.

Filonenko, V. P. & Zibrov, I. P. (2001). *Inorg. Mater.* **37**, 953–959.

Goebel, H. E. (1979). *Adv. X-ray Anal.* **22**, 255–265.

Grzechnik, A. (1998). *Chem. Mater.* **10**, 2505–2509.

Hill, R. J. & Flack, H. D. (1987). *J. Appl. Cryst.* **20**, 356–361.

Larson, A. C. & Von Dreele, R. B. (1987). Report N LA-UR-86-748. Los Alamos National Laboratory, New Mexico, USA.

Loa, I., Grzechnik, A., Schwarz, U., Syassen, K., Hanfland, M. & Kremer, R. K. (2001). *J. Alloys Compd.* **317–318**, 103–108.

McCarron, E. M. III & Calabrese, J. C. (1991). *J. Solid State Chem.* **91**, 121–125.

Minomura. S. & Drickamer. H. G. (1961). *J. Appl. Phys.* **10**, 3043–3048.

Rozier, P., Savariault, J.-M. & Galy, J. (1996). *J. Solid State Chem.* **122**, 303–308.

Suzuki, T., Saito, S. & Arakawa, W. (1977). *J. Non-Cryst. Solids*, **24**, 355–360.

Volkov, V. L., Golovkin, V. G., Fedyukov, A. S. & Zaynulin, Yu. G. (1988). *Izv. Akad. Nauk SSSR Neorg. Mater.* **24**, 1836–1840.

Werner, P.-E., Eriksson, L. & Westdahl, M. (1985). *J. Appl. Cryst.* **18**, 367–370.

Wills, A. S. & Brown, I. D. (1999). *VaList.* CEA, France.

Zibrov, I. P., Filonenko, V. P., Sundberg, M. & Werner, P.-E. (2000). *Acta Cryst.* B**56**, 659–665.

Zibrov, I. P., Filonenko, V. P., Werner, P.-E., Marinder, B.-O. & Sundberg, M. (1998). *J. Solid State Chem.* **141**, 205–211.